A DIRECTED BINDING MECHANISM OF PROCESSIVE MOTION FOR THE KINESIN MOTOR PROTEIN FAMILIES*

H. Bolterauer

Institute of Theoretical Physics
J. Liebig Universitaet Giessen, Giessen, Germany

J.A. Tuszynski

Department of Physics, University of Alberta
Edmonton, Alberta, T6G 2J1, Canada

E. Unger

Leibniz Institute for Age Research — Fritz Lipmann Institute
Department of Single Cell and Single Molecule Techniques
Beutenbergstrasse 11, 07745 Jena, Germany

(Received April 20, 2006)

Dedicated to Professor Peter Talkner on the occasion of his 60th birthday

A novel physical mechanism is discussed for the processive propagation of two-headed motor proteins such as kinesin along protein filaments. Our model uses the fact that the binding of each head must be directionality oriented to the protein filament. The binding sites are realized by a 2D periodic potential due to the filament's surface. The deviation of the geometry of the kinesin from the relaxed state to the state where both motor domains are simultaneously bound to the filament results in an internal stress of the molecule. Un-binding of one of the motor domains from the filament, which is due to the release of chemical energy from ATP hydrolysis, results in a mechanical movement until the relaxed state is reached again. We develop a simple mathematical and mechanical model in which directed binding of the heads to the filament results in a directed twist away from its relaxed state of the molecule, occurring probably in the neck linker region. Un-binding of the head from the filament relaxes the twist and defines the propagation direction. We show that there must be at least one torsional spring for every head to store elastic energy. It is the internal structure both of the relaxed and tensed-up state that defines the walking direction of kinesin. Calculations based on the model are in good quantitative agreement with experimental observations.

PACS numbers: 87.16.Ka, 87.16.Nn

* Presented at the XVIII Marian Smoluchowski Symposium on Statistical Physics, Zakopane, Poland, September 3–6, 2005.

1. Introduction

Two-headed conventional kinesin (KN) molecule walks hundreds of steps without dissociating along a microtubule (MT) before they completely dissociate from an MT [9,12,18,23]. Both heads translocate by 16 nm steps [32] and it was demonstrated that an 8 nm KN centre-of-mass movement is correlated with an ATP hydrolysis event whose rate depends on the concentration of ATP and magnesium. The maximum propagation velocity of conventional KN ranges between 0.6 mm/s and 2.0 mm/s [10, 36, 38]. For the two-headed processive KN motors, the essential force generation elements are located within each of the two globular heads [Cole and Scholey(1995),16,17]. Young *et al.*, showed that one-headed KN is often non-processive with a different mechanism of motion compared to the two-headed KN.

The movement of conventional KN along MT protofilaments could be explained by different models such as the hand-over-hand or the inchworm models [39]. Measuring stepwise motion shows that KN molecules "limp" along MTs implying that kinesin alternates conformations during its walk. The limping predicted for an asymmetric hand-over-hand mechanism is explained by axial misregistration between the α-helices of the KN neck or also by over- and under-winding of this domain [2].

We broadly classify various models into: (a) chemically-based and (b) mechanically-based ones. Especially lacking in the existing models is the inclusion of spatial dimensionality to show hand-over-hand motion of the two-headed KN since each KN head is an extended object comparable in size to the tubulin dimer. The hand-over-hand mode of propagation cannot be captured by 1D mechanical (ratchet) models which use an asymmetric MT potential [30, 31] acting on a point mass which have not been directly shown from either ab initio theory or direct experiment.

In reaction-based models chemical reactions are combined with conformational changes of the entire motor that correspond to a mechanical step. Such conformational changes represent a transition to a new relaxed state of the motor. Therefore, tensions caused by chemical reactions are relieved as driving forces for the motor. A particular type of chemical model is called a power stroke model where the motor protein's structure undergoes a conformational change driven by ATP hydrolysis.

Two types of description are used to represent biased Brownian motion in the presence of external potentials [6, 19, 20]: (a) The Langevin equation with a randomly fluctuating force [14] due to finite temperature leads to a fluctuating position behaviour. (b) The Fokker–Planck equation describes the probability of finding the mass point at a particular position in space and time. For a single mass point the Langevin equation in one dimension is

$$\gamma \frac{dx}{dt} = -\frac{dV(x)}{dx} + F(t)\,, \tag{1}$$

where x is the co-ordinate along the MT axis, $V(x)$ is the effective potential, γ is the friction coefficient and $F(t)$ the uncorrelated random force [5, 33], with

$$\langle F(t)\rangle = 0\,, \quad \left\langle F(t)F(t')\right\rangle = 2\gamma kT\delta(t-t')\,, \tag{2}$$

according to the fluctuation-dissipation theorem. The Fokker–Planck equation calculates the probability density $P(x,t)$ as [7]

$$\frac{dP(x,t)}{dt} = \partial_x \left(\left(\frac{1}{\gamma} \partial_x V(x) \right) P(x,t) + D\partial_x P(x,t) \right)\,, \tag{3}$$

where $V(x)$ is the potential and D is the diffusion coefficient $D = kT/\gamma$.

Conventional KN's directionality is mainly determined by the neck region which is also essential for processivity and regulation of ATP hydrolysis [15]. The free unattached heads for processive plus-end oriented KNs point in the walking direction [1, 21]. Thus the internal structure of the KN molecule in its relaxed state, and not an asymmetry of the binding potential of the heads, determines the KN walking direction. Since KN and other motors like Ncd have virtually the same motor domains, the differences in the walking direction between KN and Ncd appear to require a formalism that is not based on ratchet potentials.

2. Assumptions for the new model

The following considerations exclude inchworm models for movement of double-headed processive kinesin even though it is not completely excluded experimentally (for discussion see [13]). Unidirectional rotation of kinesin during movement along MTs has never been shown. Asymmetric hand over hand walking with pairs of torsion that eliminate each other after every step were found by [25]. [8] found experimental evidence that the primary working stroke of KN is closely aligned with the microtubule axis. By applying sideways loads they have shown a left/right asymmetry.

X-ray diffraction for crystallised KN shows a rotational symmetric form with a relative angle between the two heads of 120° for the "relaxed" state of the KN molecule, in the absence of MT binding or other forces acting on it [27]. By reducing the angle between the heads from 120° to zero the two heads would become collocated and co-oriented. A simultaneous binding of both heads to the same protofilament of a MT results in a tense form for the molecule as defined by probably the neck linker, a strand between core heads and the dimerisation domain that should act like a torsion spring. [1] as well as Kozielski *et al.* [28] have shown by MT decoration experiments

for a variety of KN's that the free head points into the walking direction by angles near 120° relative to the other, filament-bound, head.

However, binding of a head to the MT is only possible for a special position and direction of the head relative to the MT. Thus, we assume that each KN head exists in one of the following three chemical states:

(a) A nucleotide-free (empty) state for which a head can bind to the MT.

(b) An ATP/ATP: P state for which a head remains bound to the MT.

(c) An ADP state formed after release of P_i from ATP hydrolysis. A KN head in an ADP-state binds weakly. It is either free, or in the process of detachment from a MT; an intermediate weakly bound state can also appear.

During the mechano–chemical cycle each KN–MT complex can be found in several distinct chemical states [3], see Fig. 1:

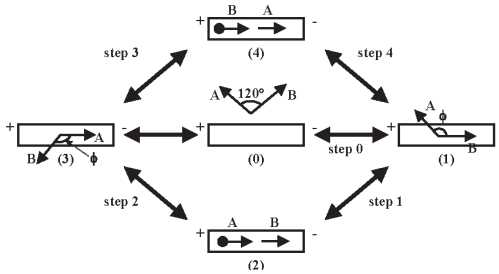


Fig. 1. The reaction cycle. Shown is the MT as square and the two heads of KN shown as arrows. Starting point is the free KN in the middle (state 0). Steps 2 and 4 are the swing out steps, where most of the movement is done.

1. Head B bound, which we assume to be in state (a), and head A, which we assume to be in state (c), pointing in the walking direction at an angle ϕ (we assume to be near 120°) to the plus direction along the MT axis.
2. Head A is in state (a), it lost ADP, and head B is in state (b); it bound ATP and possible hydrolysed it without releasing P_i, resulting in a tensed KN form. Head A is leading, head B trailing.
3. Head A bound, which we assume to be in state (a), and head B, which we assume to be, after releasing P_i in state (c), pointing in the walking direction (the plus end of MT) at an angle of ϕ to the MT axis.
4. The state is analogous to 2 with the head A in the state (b) and head B in state (a), also in a tensed KN form. Head B is leading, head A trailing.

Of cardinal importance is that chemical binding of large molecules happens only in a very precise steric position (directed binding) which means the KN/MT binding states during movement are not mirror images of each other but spatial translations. This is quite different to the human walking process, where the steps together with the feet are mirror images of each other. In our model we do not use the left-right asymmetry, but we use the forward-backward asymmetry.

It is also a model requiring twisting (torsional) degrees of freedom.

3. Description of the model

Our model employs a two-dimensional (directed) binding potential which is periodic along the MT axis. The KN motor consists of two heads and a neck/stalk. The binding of both KN heads to the MT filament must be identical in terms of both geometry and energy. The transitions between the states (steps) are described as follows:

Initially, KN is in a relaxed state unbound to a MT(with ADP in both heads).

Step 0: In the initial step one of the two heads, say head B, binds to the MT (and releases its ADP immediately). Head A is unbound (and nucleotide free), pointing in the walking direction at an angle ϕ to head B and KN ends up in state 1.

- Step 1 involves the binding of head A. Since head B remains bound the angle between the heads is 0° which requires that the KN molecule be twisted compared to its relaxed position. KN is then in state 2, with spring A loaded, spring B unloaded. (Head B binds ATP).

- In Step 2 the energy for ATP hydrolysis is used to release head B from the filament resulting in mechanical movement towards an equilibrium position state 3 which is a relaxed state for KN. This mechanical step is a swing of head B around the still bound head A. Here, the centre of mass moves by one unit of lattice periodicity, *i.e.* 8 nm for the KN–MT system (state 3).

- In Step 3 head B binds to a MT loading spring B, since head B turns counter-clockwise with respect to the correct binding direction. Therefore, KN ends up in state 4. Now spring B is loaded and spring A is unloaded.

- In Step 4, if head A is released, the mechanical step results in a swinging movement of head A around the still bound head B.

- Step 5 is identical to Step 1 and it starts a new walking cycle.

These reactions also can go backwards with reduced probability.

There must exist at least two springs, each connected to one of the two heads for this model to apply. To load the spring located at head A, with KN initially in state 1, head A turns in a clockwise direction to bind to the MT (Step 1). To load the spring located at head B, starting with state 3, head B is turned in a counter-clockwise direction to bind to the MT (Step 3).

Note that between states 1 and 3 in the cycle the neck region turns by an angle which is approximately equal to the angle between the heads in a relaxed state and a tensed state. For simplicity we choose $\phi = 120°$, the same angle between the heads in the unbound state. We further assume, and the simulation shows it, that the unbound head turns in such a way as to traverse the least path in the binding process. The ATP hydrolysis energy must exceed the binding energy, which itself must exceed the elastic spring energy.

Our model requires the use of at least eight degrees of freedom (8 position co-ordinates). The two heads have to be described by at least two mass points in order to account for directed binding. We use two spatial dimensions to see the hand-over-hand swinging motion of the two heads. Hence, we have to calculate the stochastic, two-dimensional movement of four mass points. Most of the potentials are necessary to maintain the shape of the KN molecule. Only two potentials are essential for the mechanical steps: one for the spring, which determines the swinging step and one for the binding potential to determine the binding step. These potentials specify the rate of the two reactions: binding and swinging. The corresponding energy barriers lead to the Arrhenius temperature dependence of the reaction rates.

To maintain the internal form of each head, we assume a stiff interaction between its two masses, represented by the potential functions $V_{\mathrm{h}}(\vec{r}_1 - \vec{r}_2)$ and $V_{\mathrm{h}}(\vec{r}_3 - \vec{r}_4)$ for the two heads, respectively. Then $V_{\mathrm{d}}(\vec{r}_1 + \vec{r}_2 - \vec{r}_3 - \vec{r}_4)$ is a distance dependent potential between the two centres of mass for each of the two heads. V_{h} and V_{d} are normal harmonic spring potentials with suitably chosen rest lengths. Two torsional springs are located at head A and B, respectively. When either of the heads binds to the MT with the other head already bound to it, the torsional springs in the neck linker region become loaded. There is also a binding potential between each head and a MT, denoted $V_{\mathrm{bind}}(\vec{r}_1, \vec{r}_2)$ and $V_{\mathrm{bind}}(\vec{r}_3, \vec{r}_4)$, respectively. Binding of KN to a MT is orientationally directed.

The total potential for the four mass points representing the two heads is:

$$\begin{aligned} V(\vec{r}_1, \vec{r}_2, \vec{r}_3, \vec{r}_4, \mathrm{bind}_1, \mathrm{bind}_2, \mathrm{load}) &= V_{\mathrm{h}}(\vec{r}_1 - \vec{r}_2) + V_{\mathrm{h}}(\vec{r}_3 - \vec{r}_4) \\ &+ V_{\mathrm{d}}((\vec{r}_1 + \vec{r}_2 - \vec{r}_3 - \vec{r}_4)/2) + V_{\mathrm{load}}(\vec{r}_1, \vec{r}_2, \vec{r}_3, \vec{r}_4, \mathrm{load}) \\ &+ V_{\mathrm{sA}}(\vec{r}_1, \vec{r}_2, \vec{r}_3, \vec{r}_4) + V_{\mathrm{sB}}(\vec{r}_1, \vec{r}_2, \vec{r}_3, \vec{r}_4) \\ &+ \mathrm{bind}_1\ V_{\mathrm{bind}}(\vec{r}_1, \vec{r}_2) + \mathrm{bind}_2 V_{\mathrm{bind}}(\vec{r}_3, \vec{r}_4)\,, \end{aligned} \tag{4}$$

where $V_{\mathrm{h}}(\vec{r})$ and $V_{\mathrm{d}}(\vec{r})$ are harmonic spring potentials given by

$$V_{\mathrm{h}}(\vec{r}) = C_{\mathrm{hid}}(|\vec{r}| - R_{\mathrm{hid}})^2 \tag{5}$$

and

$$V_{\mathrm{d}}(\vec{r}) = C_{\mathrm{hhd}}(|\vec{r}| - R_{\mathrm{hid}})^2 \tag{6}$$

with the following parameters used:

$$\begin{aligned} C_{\mathrm{hid}} &= 10\,kT/\mathrm{nm}^2\,, \qquad & R_{\mathrm{hid}} &= 3.6\,\mathrm{nm}\,, \\ C_{\mathrm{hhd}} &= 10\,kT/\mathrm{nm}^2\,, \qquad & R_{\mathrm{hhd}} &= 7\,\mathrm{nm}\,. \end{aligned} \tag{7}$$

The twisting spring potentials $V_{\mathrm{sA}}(\vec{r}_1, \vec{r}_2, \vec{r}_3, \vec{r}_4)$ and $V_{\mathrm{sB}}(\vec{r}_1, \vec{r}_2, \vec{r}_3, \vec{r}_4)$ only depend on the unit vectors, $\hat{n}_{\mathrm{A}}$ giving the direction of head A, $\hat{n}_{\mathrm{B}}$ giving the direction of head B, and $\hat{n}_{\mathrm{AB}}$ giving the direction between the centre of mass of head A and the centre of mass of head B. Hence

$$V_{\mathrm{sA}}(\vec{r}_1, \vec{r}_2, \vec{r}_3, \vec{r}_4) = \frac{C_{\mathrm{hh}\alpha}}{2}\,(\hat{n}_{\mathrm{AB}} \cdot M(\alpha) \cdot \hat{n}_{\mathrm{A}}) \tag{8}$$

and

$$V_{\mathrm{sB}}(\vec{r}_1, \vec{r}_2, \vec{r}_3, \vec{r}_4) = \frac{C_{\mathrm{hh}\alpha}}{2}\,(\hat{n}_{\mathrm{AB}} \cdot M(\pi - \alpha) \cdot \hat{n}_{\mathrm{B}})\,, \tag{9}$$

with

$$\hat{n}_{\mathrm{AB}} = -\frac{\vec{r}_1 + \vec{r}_2 - \vec{r}_3 - \vec{r}_4}{|\vec{r}_1 + \vec{r}_2 - \vec{r}_3 - \vec{r}_4|}\,, \quad \hat{n}_{\mathrm{A}} = \frac{\vec{r}_1 - \vec{r}_2}{|\vec{r}_1 - \vec{r}_2|}\,, \quad \hat{n}_{\mathrm{B}} = \frac{\vec{r}_3 - \vec{r}_4}{|\vec{r}_3 - \vec{r}_4|}\,. \tag{10}$$

$M(\alpha)$ and $M(\pi - \alpha)$ are rotational matrices, turning $\hat{n}_{\mathrm{A}}$ counter-clockwise and $\hat{n}_{\mathrm{B}}$ clockwise at an angle of 30°, respectively. V_{load} produces a force on the centre of mass $\vec{r}_{\mathrm{s}}$ of the whole molecule applied in the x-direction

$$V_{\mathrm{load}}(\vec{r}_1, \vec{r}_2, \vec{r}_3, \vec{r}_4, \mathrm{load}) = -C_{\mathrm{load}}\,\hat{n}_x \cdot \vec{r}_{\mathrm{s}}\,, \tag{11}$$

where

$$\vec{r}_{\mathrm{s}} = \frac{(\vec{r}_1 + \vec{r}_2 + \vec{r}_3 + \vec{r}_4)}{4}\,, \quad \hat{n}_x = \{1, 0\}\,, \quad C_{\mathrm{load}} = 10^{-21}\,\mathrm{J/nm}\,. \tag{12}$$

The binding potential has preferred directionality such that KN–MT binding is only possible in the correct direction and is given by a potential acting on the centre of mass of the head and an angle-dependent potential producing a force on the head applied in the correct direction

$$V_{\mathrm{bindA}}(\vec{r}_1, \vec{r}_2) = C_{\mathrm{hMt}} V_{\mathrm{bindm}} \left(\frac{\vec{r}_1 + \vec{r}_2}{2}\right) \left(1 + \frac{\hat{n}_x \cdot \hat{n}_{\mathrm{A}}}{2}\right)\,, \tag{13}$$

$$V_{\mathrm{bindB}}(\vec{r}_3,\vec{r}_4) = C_{\mathrm{hMt}} V_{\mathrm{bindm}} \left(\frac{\vec{r}_3+\vec{r}_4}{2}\right)\left(1+\frac{\hat{n}_x\cdot\hat{n}_{\mathrm{B}}}{2}\right), \tag{14}$$

$$C_{\mathrm{hMt}} = 25\,kT\,. \tag{15}$$

Here V_{bindm} is a potential with a period of 8 nm and a depth of one energy unit. It is a periodic continuation (period 8 nm) of the function

$$f(x,y) = -1+\frac{1}{8}\left(4+\sqrt{x^2+y^2}-\sqrt{0.01+\left(\sqrt{x^2+y^2}-4\right)^2}\right). \tag{16}$$

4. The Langevin equation formalism

We now define the individual position co-ordinates of the masses involved:

$$\vec{r}_i = \{x_i, y_i\}\,. \tag{17}$$

Then the 8 coupled Langevin equations for these co-ordinates of the four masses representing the two heads can be written as

$$\gamma\partial_t x_i = -\nabla_{x_i} V(x_1,x_2,x_3,x_4,y_1,y_2,y_3,y_4,\mathrm{bind}_1,\mathrm{bind}_2,\mathrm{load}) + F_{x_i}(t)\,, \tag{18}$$

$$\gamma\partial_t y_i = -\nabla_{y_i} V(x_1,x_2,x_3,x_4,y_1,y_2,y_3,y_4,\mathrm{bind}_1,\mathrm{bind}_2,\mathrm{load}) + F_{y_i}(t)\,, \tag{19}$$

where γ is the friction constant which is judiciously chosen as $\gamma = 6\times 10^{-11}$kg/s. Here, $F_{x_i}(t)$ and $F_{y_i}(t)$ define random forces satisfying the usual conditions:

$$\begin{aligned}
\langle F_{x_i}(t)\rangle &= 0\,,\\
\langle F_{y_i}(t)\rangle &= 0\,,\\
\langle F_{x_i}(t)F_{y_j}(t')\rangle &= 0\,,\\
\langle F_{x_i}(t)F_{x_j}(t')\rangle &= 2\gamma kT\delta_{i,j}\delta(t-t')\,,\\
\langle F_{y_i}(t)F_{y_j}(t')\rangle &= 2\gamma kT\delta_{i,j}\delta(t-t')\,.
\end{aligned} \tag{20}$$

The above coupled Langevin equations were solved numerically. The mechanical steps described above arise naturally if we switch the binding of head A and B on and off, given by $m = \{\mathrm{bind}_1, \mathrm{bind}_2\}$. For state 1 we have: $m = \{0,1\}$. Independently of the initial condition, we find head B bound and head A unbound. Note that head A does not show the exact angle of 120° with respect to head B because of thermal fluctuations. The following three figures describe the centre of mass of the KN, the centres of mass of the two heads and the position of one head, resulting from the same calculation, showing the first 6 steps of the molecule's motion. Fig. 2 shows the calculated position of the total centre of mass of the two heads in the

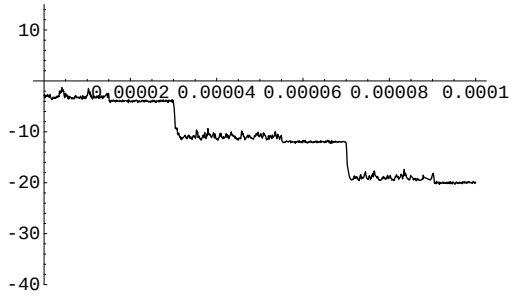


Fig. 2. A time series diagram representing the calculated position *versus* time function of the centre of mass of KN.

x-direction, which is the direction along the MT for the first 6 steps of the movement. Unless binding occurs for a given head, the fluctuations of the head position are fairly large. Fig. 3 shows the calculated positions of the centres of mass of the two heads in the x-direction, which is the direction along the MT. It is clear that hand-over-hand movement takes place in the direction from the −end to the +end of the MT.

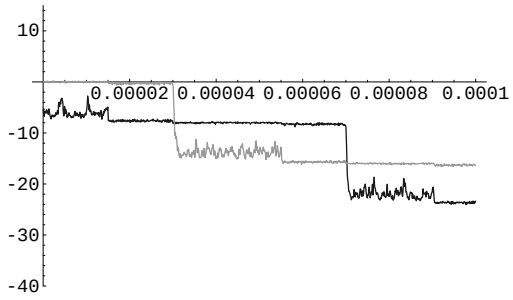


Fig. 3. A time series diagram representing the calculated position *versus* time function of the two heads comprising a KN molecule.

In Fig. 4 we show the calculated x co-ordinates of the two mass points of head A. In these graphs the load force is assumed to be zero. Fig. 5 shows the same calculated walking cycle in two dimensions. We see the alternating twists of head A and B first shown in [11]. Individual computations produce somewhat different graphs, because the random force is different in every run.

The Langevin approach presented above has two major shortcomings. The binding parameters bind_1, bind_2 follow the following simple rules. First, we switch the binding force in a regular fashion. We start with (a) $m = \{0, 1\}$, *i.e.* head B binds, this automatically means that head A is leading

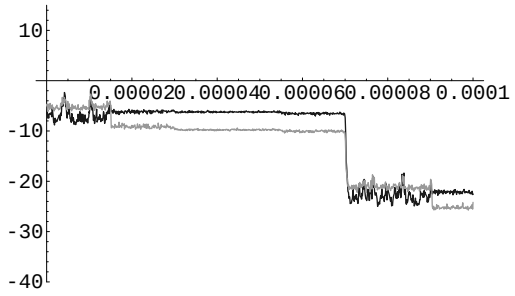


Fig. 4. The calculated position co-ordinates of head A: x_1 and x_2 as a function of time.

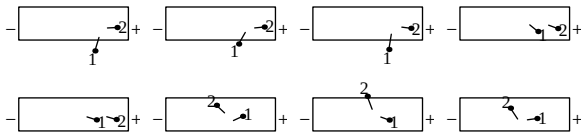


Fig. 5. A schematic drawing of the KN walking cycle in two dimensions.

for the moment. Then (b) $m = \{1, 1\}$, *i.e.* both heads bind with head A leading with its spring loaded. We assume that only the head with an empty spring can unbind which is the trailing head. This gives (c) $m = \{1, 0\}$. The unrealistic aspect in this case is that we switch from (a) to (b) to (c) in an orderly way at fixed time intervals. The second shortcoming of this Langevin calculation is that the energy barriers for the binding and unbinding processes are not included in this simulation.

5. A combination of the Fokker–Planck equation and the rate equation

The Langevin approach shows the geometry of the walking process, but does not include the transition rates for hydrolysis events during which the KN heads lose ADP. The chemical processes of binding and unbinding were included by simply switching a attractive binding potential on and off. Most importantly for binding, the two complicated surfaces must fit into each other in a specific relative steric configuration. This requires a complicated path which the head must traverse before it can bind to MT. The end of this path will be on the binding site, but before binding occurs, the head will be effected by repulsive forces resulting in the presence of effective energy barriers.

To illustrate this idea Fig. 6 shows a molecules, assumed to be a point mass, while a second (larger) molecule's surface is shown as a complicated curve. The particle has to search its way through the labyrinth of the surface area of the large molecule before it can find a binding site. Only with help of thermal fluctuations can the particle reach the desired binding site. These effects affect the temperature dependence of the chemical reaction in a characteristic way.

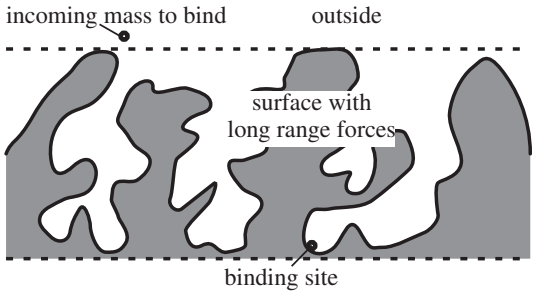


Fig. 6. A small molecule, coming from the outside has to find its way through the surface area of a large molecule until it finds the binding site.

A crude approach to deal with these effects is the introduction of an energy barrier, resulting in the famous Arrhenius temperature dependence of transition rates for chemical processes

$$k = A \exp\left(-\frac{E_\mathrm{b}}{kT}\right) . \tag{21}$$

We can now calculate the probability of finding the system in a particular state. A state is defined by the continuous 8 co-ordinates of the four mass points R and the discrete binding parameters m

$$R = \{x_1, x_2, x_3, x_4, y_1, y_2, y_3, y_4\} , \quad m = \{\mathrm{bind}_1, \mathrm{bind}_2\} , \tag{22}$$

where m has the three possible values

$$m = \{1,1\}, \{1,0\}, \text{ or } \{0,1\} . \tag{23}$$

$W(R,m,t)$ is the probability density for a certain time t that the co-ordinates have the value R, and the binding parameters are m. The equation of motion for $W(R,m,t)$ is the extended Fokker–Planck equation,

$$\begin{aligned} \partial_t W(R,m,t) \;=\; & \nabla \cdot ((\nabla V(R,m) W(R,m,t) + D \nabla W(R,m,t)) \\ & + \sum_{n(n\neq m)} (-\Omega_{mn}(R) W(R,m,t) + \Omega_{nm}(R) W(R,n,t)) . \end{aligned} \tag{24}$$

Here D is the diffusion coefficient $D = kT/\gamma$. ∇ is the 8 dimensional gradient operator. $\Omega_{mn}(R)$ are the transition probabilities for the different binding parameters. $V(R,m)$ is the effective potential, which also depends on the load plus a barrier potential

$$\begin{aligned} V(R,m) &= V(x_1,x_2,x_3,x_4,y_1,y_2,y_3,y_4,\mathrm{bind}_1,\mathrm{bind}_2,\mathrm{load}) \\ &\quad + V_{\mathrm{barrier}}(x_1,x_2,x_3,x_4,y_1,y_2,y_3,y_4,\mathrm{bind}_1,\mathrm{bind}_2)\,. \end{aligned} \tag{25}$$

There appears to be no mathematical method (analytical or numerical) of solving this Fokker–Planck rate equation for our model, even if we only need the stationary solution since it is a system of 8-dimensional PDE. In the one-dimensional case, a similar equation with some further simplifications was solved by [29].

To calculate the velocity of KN within our model we divide the whole reaction cycle into individual steps and calculate their transition rates. This calculation is too complicated in general due to the high dimensionality of the system. But there is one exception when we focus only on the most important mechanical step. The swinging step starts with state 4, in which both heads are bound $m = \{1,1\}$ and spring B is loaded. When head A is released, it swings around head B until an angle of approximately 120° is reached. This, however, is a quasi-one-dimensional movement for the centre of mass of head A, the path of which is a circle around head B. Perpendicular fluctuations are now neglected, since we chose the distance potential V_{d} as very stiff. A similar idea of neglecting non-essential degrees of freedom can be found in [26]. The effective time-dependent co-ordinate is the arc length of the circle, s.

The Fokker–Planck equation for this one-dimensional movement of head A then reads:

$$\partial_t W(s,t) = \partial_s((\partial_s V_1(s))W[s,t] + D\partial_s W(s,t))\,. \tag{26}$$

Here, the one-dimensional potential $V_1(s)$ contains three separate potential terms: the spring potential of head B, the load potential and the energy barrier term. The spring potential as a function of s is:

$$V_{\mathrm{sB}}(s) = -\frac{1}{2}\cos\left(\frac{s-s_0}{R_{\mathrm{hhd}}}\right) C_{\mathrm{hh}\alpha}\,. \tag{27}$$

The load potential in terms of its dependence on s reads

$$V_1(s,\mathrm{load}) = \left[1-\cos\left(\frac{s}{R_{\mathrm{hhd}}}\right)\right] C_{\mathrm{load}} R_{\mathrm{hhd}}\,. \tag{28}$$

The swinging motion is combined with a chemical reaction, *i.e.* the release of head A, which is sensitive to its potential energy barrier, so we have to

add a chemical reaction potential $V_{\mathrm{R}}(s)$, *i.e.* the barrier potential, which we define as

$$V_{\mathrm{R}}(s) = E_{\mathrm{B}} \exp\left(- \left[\frac{(s - s_1)}{2} \right]^2 \right) \tag{29}$$

to obtain

$$V_1(s) = V_{\mathrm{sB}}(s) + \mathrm{V}_1(s) + V_{\mathrm{R}}(s)\,. \tag{30}$$

The barrier energy E_{sB} and the location co-ordinate s_1 of the barrier are essential. Only with V_{sB} the total potential $V(s)$ has two minima corresponding to the initial state and the final state. Fig. 7 shows $V(s)$ with and without V_{sB}. The constants are chosen as $E_{\mathrm{sB}} = 10\,kT$ and $s_1 = 7\,$.

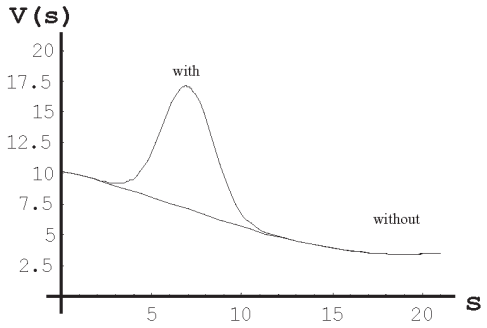


Fig. 7. The one-dimensional "swing out" potential V_{s} with and without the energy barrier.

To calculate the corresponding reaction rates we use Kramer's escape rate, where

$$k_{\mathrm{swing}} = \frac{kT}{\gamma} \left[\left(\int\limits_{\mathrm{int}_1} \exp(-V(s)kT) ds \right) \int\limits_{\mathrm{int}_2} \exp\left(\frac{V(s)}{kT} \right) ds \right]^{-1} . \tag{31}$$

Here, the first integral (int_1) has to be calculated around the starting minimum of $V(s)$ (the initial state), the second integral (int_2) around the maximum of $V(s)$ (the energy barrier). We then calculated k_{swing} in both directions and combined it with the other reaction rates of the chemical cycle used.

For the other steps we use the reaction cycle given by Howard [22] and Hirose *et al.* [21] consisting of three different reactions. We start with head A in an ADP state unbound from a MT and head B in an empty state bound to the MT. In reaction 1 head B binds an ATP complex. In reaction 2 head A loses the ADP and binds also to the MT. In reaction 3 head B hydrolyses ATP, unbinds and makes the swing.

Reactions 1 and 2 have the rates $k_1^+(F)$, $k_1^-(F)$, and $k_2(F)$, respectively. Reaction 3 can go in both directions, which we calculated as $k_{+\mathrm{swing}}(F)$ and $k_{-\mathrm{swing}}(F)$ using the Kramers escape method. For the first reaction (binding of ATP with rates $k_1^+(F)$, $k_1^-(F)$) and the second reaction (double binding to MT, with rate $k_2(F)$), we use similar rate constants as in Howard [22]. The stationary reaction equations for this reaction cycle read

$$P_2 k_1^- - P_1 k_{\mathrm{swing}}^- - [\mathrm{ATP}] P_1 k_1^+ + P_3 k_{\mathrm{swing}}^+ = 0\,, \tag{32}$$

$$-P_2 k_2 - P_2 k_1^- + [\mathrm{ATP}] P_1 k_1^+ = 0\,, \tag{33}$$

$$P_2 k_2 + P_1 k_{\mathrm{swing}}^- - P_3 k_{\mathrm{swing}}^+ = 0\,, \tag{34}$$

where P_1, P_2, P_3 are the probabilities to find the system in states 1, 2, 3 and [ATP] is the concentration of ATP. Only two of these equations are linearly independent and we have the normalisation condition

$$P_1 + P_2 + P_3 = 1\,. \tag{35}$$

We then calculate the current j

$$j = k_2 P_2 \tag{36}$$

and multiplying j by the step-length of 8 nm we obtain the velocity v as

$$v = \frac{8[\mathrm{ATP}] k_2 k_1^+ k_{\mathrm{swing}}^+}{[\mathrm{ATP}] k_1^+ k_{\mathrm{swing}}^+ + k_1^- (k_{\mathrm{swing}}^- + k_{\mathrm{swing}}^+) + k_2 (k_{\mathrm{swing}}^- + [\mathrm{ATP}] k_1^+ + k_{\mathrm{swing}}^+)}\,. \tag{37}$$

After one of the heads unbinds, the forces on the head are working only on its centre of mass. Therefore, the Fokker–Planck equation for this process is that of a two-dimensional particle in a given potential. We used our potential and solved the equation numerically starting with a Gaussian distribution for the density distribution. Some steps in the time development are shown in Fig. 8.

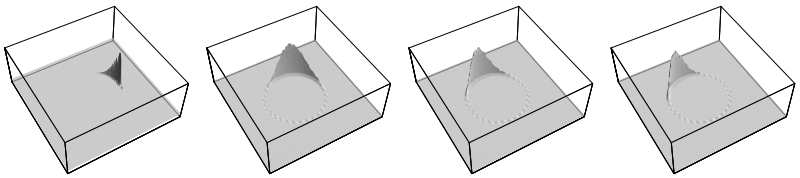


Fig. 8. The time development of the probability distribution, the time is going from left to right.

To test our model we have calculated the force-velocity relationship for a number of ATP concentrations corresponding to several experimental data sets. We use Eq. (39) together with $k^{-}_{\text{swing}}(F)$ and $k^{+}_{\text{swing}}(F)$ calculated with the help of Eq. (33)

$$\begin{aligned} k_1^+(F) &= 100e^{-1.120716F}\,, \\ k_1^-(F) &= 3000\,e^{1.120716F}\,, \\ k_2(F) &= 100\,e^{-0.241432F}\,. \end{aligned} \tag{38}$$

We show the comparison in Figs. 9–11. Our results are given by the solid black line, while those calculated by [22] are shown as a dashed line. Figs. 9 and 10 compare with experiments done by Visscher *et al.* [37]. Fig. 11 compares our results with an experiment by [35]. The agreement achieved between our model and experiment especially for low ATP concentrations is very good. While our simulations resulted in a mode of propagation that is reminiscent of the hand-over-hand motion, it has not required a pronounced rotation of the stalk region as has been recently reported based on experiments [24].

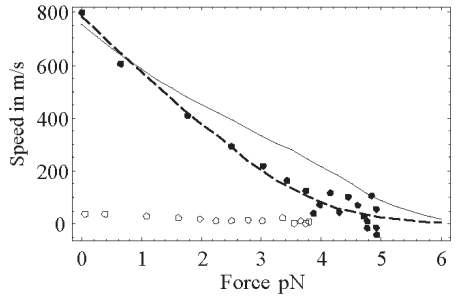


Fig. 9. The force-velocity curve for kinesin at the concentration of [ATP] = 600 μM.

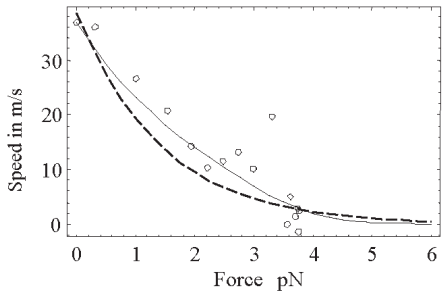


Fig. 10. The force-velocity curve for kinesin at the concentration of [ATP] = 1.5 μM.

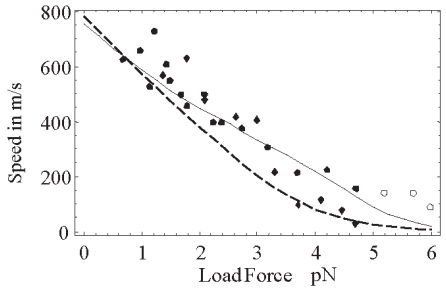


Fig. 11. The force-velocity curve for kinesin at the concentration of [ATP] $\gg 90\,\mu$M.

Many papers using ratchet models and Brownian motors [4, 19, 20, 34], to explain the behaviour of molecular motors like kinesin resulted in a directional motion of the motor. In the usual ratchet models this is explained with an asymmetry of the ratchet potential. Our model stresses that the binding of the heads to MT must be directed. This together with the fact that the geometric form of the relaxed kinesin is symmetric, makes our model directional.

To make it clear that our model does not describe a Brownian motor we take away any thermal fluctuation ($T = 0$), which means we solve the Langevin equation without any random force, so it cannot violate the second law of thermodynamics. The unbinding of one of the two heads happens after certain fixed intervals, the time in which the ATP complex binds to the head and ATP hydrolysis occurs. The unbinding of one of the two heads occurs in this calculation with an equal probability. After a head unbinds, it can bind again after a characteristic time, this is just the time it takes the head to lose its ADP and become an empty head again. The result of this simplified calculations is shown in Fig. 12. If the leading head (the wrong head) unbinds, it binds again later at the same spot as before. If the trailing

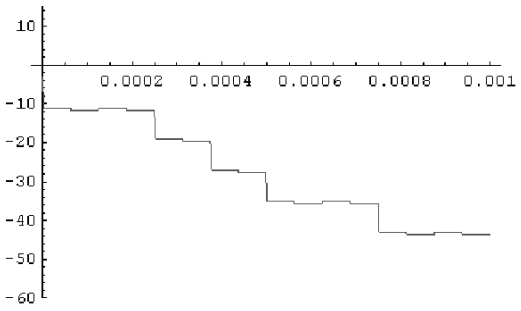


Fig. 12. A simplified calculation without temperature, but with equal probabilities for both heads to unbind.

head (the right head) unbinds, it swings around and binds again later at a new spot 16 nm away from the old one. Note that "wrong steps" can be seen for this example around $t = 0.0006$.

6. Discussion

We developed a theoretical model for kinesin using the geometrical structure of the molecule. It is a mechanical model, since we use the difference between relaxed and tensed states and describe them by springs. We show that there must exist at least two springs. The movement of kinesin is stochastic, but kinesin is a chemically reactive molecule. A chemical binding of extended molecules must be directed and from this, we can explain quite naturally, the loading and reloading of the two springs, which results in an asymmetric hand-over-hand movement described by experiments. Furthermore, for chemical binding processes energy barriers are required. The well known Arrhenius equation, describing the temperature dependence of chemical reaction rates, is a typical result of energy barriers. We solved the requisite Langevin equations to show the geometrical hand-over-hand movement. We estimated the transition rate for the swing out step, which we used to solve a system of rate equations and calculated the velocity depending on the load, which was compared with experimental data given by literature.

In summary, our model is not a model of a Brownian motor since it is not using ratchet potentials. The directionality is given by the internal structure of the kinesin molecule. The angle ϕ determines the direction of the walk and we predict that changing ϕ would change the direction of the walk. The energy flow is clearly defined in our model: for the second head to bind, if the first is already bound, it has to turn around, loading its spring, which means positive potential spring energy is stored together with the negative binding energy, then ATP hydrolysis and release of P_i at the trailing head pumps energy into the system, the energy used to break the binding of this head from the MT; the remaining spring energy of the leading head is free to cause the "hand-over-hand" swing-out process as a biased random walk. This storing of potential energy seems to be very important. The binding forces are short range, hence they cannot cause the walking over such distances directly. The system is over-damped so molecules must be propelled ballistically. Instead, ATP hydrolysis causes unbinding; in other words there is an increase of potential energy. The system always tends to go in the direction to reach the minimum of the potential energy. The walking direction is given by the internal structure of KN.

Finally, we make several predictions regarding the outcome of future experiments when the angle ϕ could be controlled by experimenting with the structure of the neck linker region. The case when ϕ is approximately

120° was discussed in this paper. For $\phi = 180°$ (both heads are oriented anti-parallel outwards) there is no change in the walking direction but the alternating swinging direction can be distorted. If we reduce ϕ to 0° (both heads are oriented parallel) the movement is expected to be similar to a random walk, there is no symmetry breaking and, therefore, no preferred walking direction. If ϕ is further reduced to negative values (both heads are oriented inwards instead of outwards), we have the same scenario as before, except the direction of walking is now reversed. We conclude that our model could also be a starting point for the description of Ncd.

We believe that the model presented here for the directed walk of double-headed processive kinesins, could also be used for description of processive myosin walks, which will be part of our future work.

REFERENCES

[1] I. Arnal, R.H. Wade, *Structure* **6**, 33 (1998).

[2] C.L. Asbury, A.N. Fehr, S.M. Block, *Science* **302**, 2130 (2003).

[3] C.L. Asbury, *Curr. Opinion Cell Biol.* **17**, 89 (2005).

[4] R.D. Astumian, P. Hänggi, *Phys. Today* **55(11)**, 33 (2002).

[5] R.D. Astumian, M. Bier, *Phys. Rev. Lett.* **72**, 1766 (1994).

[6] R.D. Astumian, *Science* **276**, 917 (1997).

[7] M. Bier, R.D. Astumian, *Bioelectrochem. Bioenerg.* **39**, 67 (1996).

[8] S.M. Block, C.L. Asbury, J.W. Shaevitz, M.J. Lang, *PNAS USA* **100**, 2351 (2003).

[9] S.M. Block, L.S. Goldstein, B.J. Schnapp, *Nature* **348**, 348 (1990).

[10] K.J. Boehm, P. Steinmetzer, A. Daniel, W. Vater, M. Baum, E. Unger, *Cell Motil. Cytoskeleton* **37**, 226 (1997).

[11] H. Bolterauer, J.A. Tuszynski, *Int. J. Nonlinear Sci. Num. Sim.* **3**, 185 (2002).

[Cole and Scholey(1995)] D.G. Cole, J.M. Scholey, *Trends Cell. Biol.* **5**, 259 (1995).

[12] I.M. Crevel, A. Lockhart, R.A. Cross, *J. Mol. Biol.* **273**, 160 (1997).

[13] R.A. Cross, *Curr. Biol.* **14**, 158 (2004).

[14] C.R. Doering, W. Horsthemke, J. Riordan, *Phys. Rev. Lett.* **72**, 2984 (1994).

[15] S.A. Endow, *Molecular Motors*, Wiley-VCI, Weinheim (2003), chap. Molecular Motor Directionality.

[16] D.D. Hackney, *Nature* **376**, 215 (1995).

[17] D.D. Hackney, *Annu. Rev. Physiol.* **58**, 731 (1996).

[18] W.O. Hancock, J. Howard, *J. Cell Biol.* **140**, 1395 (1998).

[19] P. Hänggi, F. Marchesoni, *Chaos* **15**, 026101 (2005).

[20] P. Hänggi, F. Marchesoni, F. Nori, *Ann. Phys.* (Leipzig) **14**, 51 (2005).

[21] K. Hirose, U. Henningsen, M. Schliwa, C. Toyoshima, T. Shimizu, M. Alonso, R.A. Cross, L.A. Amos, *EMBO J.* **19**, 5308 (2000).

[22] J. Howard, Mechanics of Motor Proteins and the Cytoskeleton, Sinauer Associates Inc., Sunderland, Mass. (2001).

[23] J. Howard, A.J. Hudspeth, R.D. Vale, *Nature* **342**, 154 (1989).

[24] W. Hua, J. Chung, J. Gelles, *Science* **295**, 844 (2002).

[25] K. Kaseda, H. Higuchi, K. Hirose, *Nature Cell Biol.* **5**, 1079 (2003).

[26] D. Keller, C. Bustamante, *Biophys. J.* **78**, 541 (2000).

[27] F. Kozielski, S. Sack, A. Marx, M. Thormälen, E. Schönbrunn, V. Biou, A. Thompson, E.-M. Mandelkow, E. Mandelkow, *Cell* **91**, 985 (1997).

[28] F. Kozielski, I. Arnal, R.H. Wade, *Curr. Biol.* **8**, 191 (1998).

[29] R. Lipowsky, T. Harms, *Eur. Biophys. J.* **29**, 542 (2000).

[30] M.O. Magnasco, *Phys. Rev. Lett.* **71**, 1477 (1993).

[31] M.O. Magnasco, *Phys. Rev. Lett.* **72**, 2656 (1994).

[32] E. Mandelkow, K.A. Johnson, *Trends Biochem. Sci.* **23**, 429 (1998).

[33] J. Prost, J.F. Chauwin, L. Peliti, A. Ajdari, *Phys. Rev. Lett.* **72**, 2652 (1994).

[34] P. Reimann, *Phys. Rep.* **361**, 57 (2002).

[35] K. Svoboda, S.M. Block, *Cell* **77**, 773 (1994).

[36] R.D. Vale, T.S. Reese, M.P. Sheetz, *Cell* **42**, 39 (1985).

[37] K. Visscher, M.J. Schnitzer, S.M. Block, *Nature* **400**, 184 (1999).

[38] A. von Massow, E.M. Mandelkow, E. Mandelkow, *Cell. Motil. Cytoskeleton* **14**, 562 (1989).

[39] A. Yildiz, P.R. Selvin, *Trends Cell Biol.* **15**, 112 (2005).

[40] E.C. Young, H.K. Mahtani, J. Gelles, *Biochemistry* **37**, 3467 (1998).